Grazing-angle intersubband absorption in *n*-doped GaAs multiple quantum wells

E. Dupont,* M. Gao, H. C. Liu, Z. R. Wasilewski, and A. Shen
Institute for Microstructural Sciences, National Research Council, Ottawa, Ontario, Canada K1A 0R6

M. Załużny
Institute of Physics, M. Curie Sklodowska University, pl. M. Curie Sklodowskiej 1, 20-031 Lublin, Poland

S. R. Schmidt and A. Seilmeier
Institute of Physics, University of Bayreuth, 95440 Bayreuth, Germany
(Received 20 December 1999)

We present a study of the mid-infrared intersubband absorption in *n*-doped GaAs/$Al_xGa_{1-x}As$ multiple quantum wells (MQWs) for various internal incident angles. Above 45° incidence we show that the traveling-wave approximation is not valid: redshifts of the absorption peak are observed, strikingly additional peaks appear for thick structures, and the strength of absorption does not necessarily increase with the incident angle. The understanding of such complex absorption behavior requires considering the quantum well as an absorbing uniaxial material and taking into account the multiple reflections of the light inside the MQW.

The intersubband absorption in multiple-quantum-well (MQW) structures has been studied intensively. *n*-doped quantum wells (QWs) are uniaxial materials featuring a mid/far-infrared (IR) absorption for light polarized perpendicular to the layers. Provided the absorption is strong, the low-coupling Brewster angle configuration is commonly used to measure the intersubband absorption. In this low-efficient-coupling scheme, the traveling-wave approximation (TWA) is usually applied to this multilayer anisotropic material. The intersubband resonance peak observed at the Brewster angle corresponds to the splitting energy E_{21} between the first two subbands modified by collective effects during the absorption process (depolarization and exciton shifts).[1] The magnitude of the absorption line at the Brewster angle gives good insight into the intersubband susceptibility. Under this approximation the IR absorbance is proportional to the number of wells, the intersubband susceptibility, and the coupling factor $\sin^2\varphi/\cos\varphi$, where φ is the angle of incidence within the sample.

The traveling-wave approximation at the Brewster angle is valid up to a maximum product between the oscillator strength and the average doping density in the QW of about $10^{17}\,\mathrm{cm}^{-3}$. Above this limit, the refraction law in QWs, as dictated by the ellipsoid of indices, will induce a blueshift of the imaginary part of the wave vector inside the QWs and a significant change for its real part. Consequently, after multiple reflections of the light inside the heterostructure, the peak of the intersubband absorption will appear at slightly different energy than the depolarization-shifted transition energy E_{21}. The refraction law in uniform uniaxial materials is represented by the equation

$$k_0^2=\frac{k_z^2}{n_0^2+\chi_D}+\frac{k_x^2}{n_0^2+\chi_{\mathrm{ISB}}}, \tag{1}$$

where k_0 is the wave vector in vacuum and k_z and k_x are the wave vector projections inside the QWs, in the directions perpendicular and parallel to the layers, respectively. The projection k_x is an invariant during the propagation of the light in the structure and it is fixed by the incident angle. The variable n_0 stands for the ordinary index of the well material. The intersubband (intrasubband) susceptibility $\chi_{\mathrm{ISB}}(\chi_D)$ modulates the index of the two-dimensional (2D) electron gas along the growth axis z (in the QW plane).[2]

For high-coupling configurations such as zigzag waveguides,[3,4] a strong intersubband susceptibility can induce evanescent waves in the QWs which lead to significant reflections of the light at the well/barrier interfaces. Załużny and Nalewajko[5] predicted that the multiple reflections inside the MQW structure will be able to modify the absorption spectrum significantly, especially for thick structures. Their model also shows that the absorption spectrum depends strongly on the different ordinary indices in the well and barrier. With the $\varphi>45°$ zigzag configuration, a large number of wells, and a strong intersubband susceptibility, a redshift of the observed resonant absorption is predicted. For very thick MQW structures and for specific incident angles φ of the light onto the QWs, satellite peaks far detuned from the resonance E_{21} are also expected. Qualitatively, the redshift can be explained by the strong decrease of the real part of the extraordinary dielectric constant when the photon energy is higher than E_{21}.[6] At grazing angles φ, Eq. (1) shows there is a wide region of photon energy above the quantum resonance E_{21} for which the imaginary part of k_z is higher than its real part: in other words, the wave is mainly evanescent in the QWs. If the MQW is thick, and if the multiple reflections are neglected, the IR light will not propagate easily through the structure and, as a result, the absorption will be strongly reduced in this spectral range. Figure 1 illustrates this effect in the particular case of a square quantum well with a 100 meV depolarization-shifted resonance E_{21}. A Q factor of the intersubband oscillator of 10 was chosen, meaning that, at the Brewster angle, the full width at half maximum (FWHM) of the absorption spectrum is 10 times smaller than the photon energy at the absorption peak. The average carrier concentration in the well is $4\times10^{17}\,\mathrm{cm}^{-3}$.

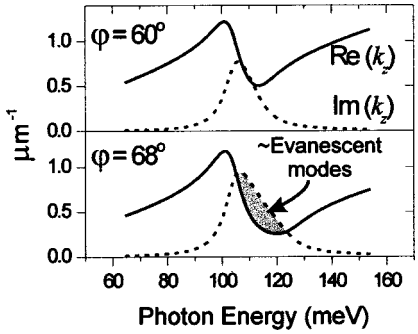

FIG. 1. Simulated projection of the wave vector along the growth axis of a GaAs quantum well for two internal incident angles φ in the GaAs substrate. The quantum resonance is fixed at 100 meV, and the Q factor of the infrared oscillator is 10. The dashed lines represent the imaginary part of k_z, the solid lines its real part.

The figure shows the real and imaginary parts of k_z inside the QW for two incident angles in the GaAs substrate. However, this simple interpretation with evanescent waves is incomplete: it shows only the spectral range where deviations from the TWA can be expected and it forgets that evanescent waves can induce significant reflections of the light at the well/barrier interfaces. To predict quantitatively the intersubband absorption it is essential to include the multiple reflections due to these evanescent modes; this can be done via a multilayer calculation in uniaxial media (the local approach) or by using an effective-medium approach.[5] The simulations show that the multiple reflections of the light between the well/barrier interfaces can shift the apparent resonance and, in certain conditions, they can induce additional absorption lines. The electromagnetics of this problem is such that the interpretation of these features in an intuitive picture is rendered difficult.

Experimentally, the intersubband absorption in zigzag waveguides has not been studied and analyzed in detail. In thin MQW structures Kane *et al.*[7] and Schneider *et al.*[8] demonstrated the importance of interference between the incident and reflected waves at the semiconductor/metal and semiconductor/air interfaces. For thick structures and for large internal incident angles φ, the TWA is normally used. However, in a sum-frequency generation experiment,[9] it was shown that multiple reflections of the pump light inside the MQW at $\varphi=77°$ had to be taken into account. More generally, the effect of multiple reflections could be important to determine the optimum conditions in nonlinear optical experiments using intersubband transitions.[10] Also, the understanding of intersubband absorption at grazing angle is highly beneficial for the optimization of quantum-well infrared photodetectors (QWIPs), where the IR light is coupled through diffractive gratings. Experimentally, it has been found that the optimum grating at the peak wavelength hc/E_{21} is obtained at a diffraction angle φ such that $\sin\varphi \sim 0.9$.[11,12] The inefficiency of $\sin\varphi \approx 1$ diffraction gratings is attributed to the rapid cutoff of the grating at longer wavelengths. Would it be possible to explain the failure of these gratings by multiple-reflection effects inside the MQW?

Detailed intersubband absorption measurements at grazing angle have been performed on two wafers (*A* and *B*) grown by molecular-beam epitaxy on a semi-insulating GaAs (001) substrate. These wafers were chosen to test the theoretical predictions of Ref. 5: they contain a large number of QWs, they do not have contacting layers as in QWIPs, and the transitions are bound to bound. Unlike in the simulation of Ref. 5 the quantum wells of wafers *A* and *B* are not square wells. However, the difference of indices of refraction between the barrier and the intermediate barrier is too small to induce large changes in IR absorption.

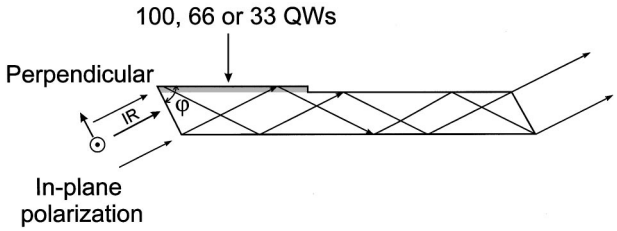

FIG. 2. Schematic of a φ^0 zigzag waveguide used for wafer *A*. The IR light is at normal incidence onto the polished facet. There is only one reflection at the MQW/air interface and the length and thickness are such as to obtain maximum infrared throughout.

Sample *A* is a 100-repeat quantum-well structure. Each period consists of a 200 Å $Al_{0.3}Ga_{0.7}As$ barrier, an 80 Å GaAs well with a Si δ doping of $5\times10^{11}\,cm^{-2}$, a 56 Å $Al_{0.3}Ga_{0.7}As$ intermediate barrier, and a 67 Å $Al_{0.15}Ga_{0.85}As$ satellite well. By design, the first excited state of the wide quantum well, $E1_w$, is approximately in resonance with the ground state of the satellite well $E0_s(E1_w=E0_s)$. Because of the weak-tunneling coupling through the intermediate barrier the anticrossing between these levels is only 5 meV. At the Brewster angle and for *p*-polarized infrared light, a single Lorentzian absorption line was observed at 128 meV with 8% peak value. Actually, the Lorentzian shape suggests that the relative position between $E1_w$ and $E0_s$ is not appropriate to obtain the anticrossing at zero electric field. Indeed, it has been theoretically demonstrated that the exact anticrossing at zero field occurs when $E0_s=E1_w+\Delta E$, where ΔE is the depolarization shift.[13]

Sample *B* is the same as that reported in Ref. 9. It is a 200-repeat step quantum-well structure, each period consisting of (60 Å GaAs)-(45 Å $Al_{0.09}Ga_{0.91}As$) and a 300 Å $Al_{0.39}Ga_{0.61}As$ barrier. The nominal carrier concentration is $1.2\times10^{12}\,cm^{-2}$. At the Brewster angle, a 22% absorption peak centered at 111 meV due to the intersubband $E1\rightarrow E2$ transition is measured.

With wafer *A*, four $4\times12\,mm^2$ zigzag waveguides were made with $\varphi=45°$, 60°, 70°, and 80° (Fig. 2). Mesas were etched to define a region interacting with the IR radiation. The length of the mesas and the total length of the four samples are such that a maximum throughput is obtained with only one reflection at the MQW/air interface. On these samples two 4-mm-wide stripes were etched to study the absorption of 100, 66, and 33 QWs. Sample *B* was simply processed as a 60° zigzag waveguide without optimizing the length and thickness. The intersubband absorption is measured with a Fourier transform infrared spectrometer. The polarized infrared beam is focused onto the polished facet of the samples with an $f/10$ effective numerical aperture optics; the transmitted beam is recorded with a HgCdTe-cooled detector. The in-plane polarization spectra are used as references. The samples are mounted on the axis of a rotation

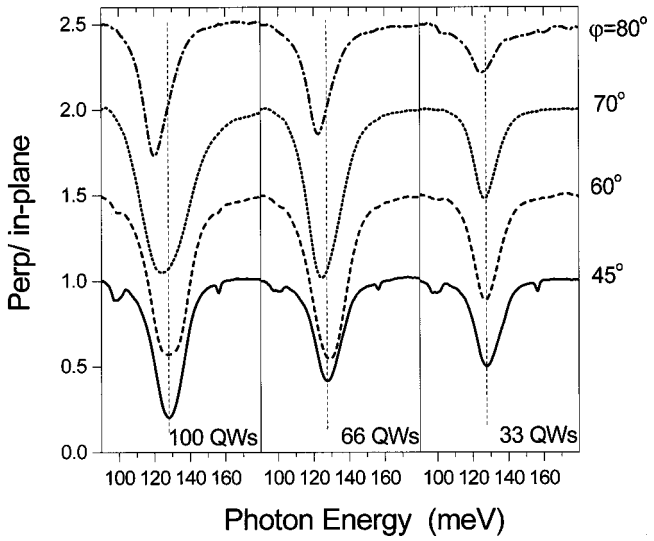

FIG. 3. Room-temperature transmittance spectra on wafer *A* at four internal incident angles φ and three thicknesses of the MQWs. For clarity, the spectra are vertically shifted by 0.5. The vertical dashed lines are drawn to guide the eye.

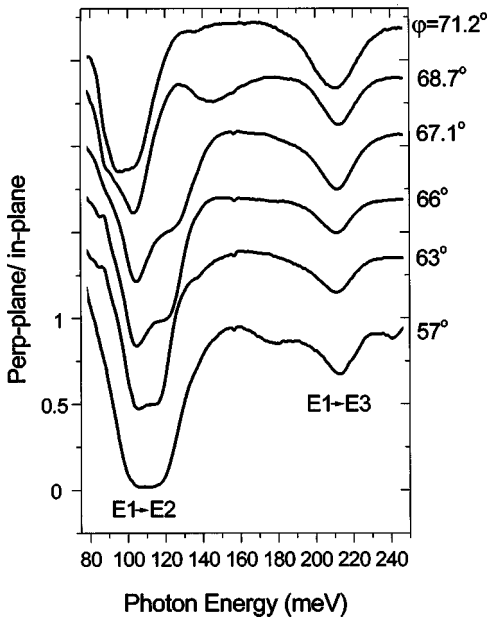

FIG. 4. Room-temperature transmittance spectra on wafer *B* at six internal incident angles. For clarity, the spectra are vertically shifted by 0.35.

stage for adjustment of the incident angle. The polished facets of sample *A* are illuminated at normal incidence. For sample *B*, the angle of incidence onto the 60° facet is adjusted from 40° to −10° so that, internally, the grazing angle φ varies from 71.2° to 57°. The $f/10$ focusing optics means that, internally, the incident angle onto the QWs varies within $\sim\pm1°$.

Figure 3 represents the experimental results of wafer *A*, for the four sets of waveguides and the three MQW thicknesses. For the three MQW thicknesses the maximum integrated absorption is obtained between $\varphi=60°$ and 70°. At large angle ($\varphi=80°$, $\sin\varphi=0.98$) there is a clear decrease of absorption. This observation is consistent with the inefficiency of $\sin\varphi\approx1$ diffraction gratings in QWIPs. With 100 and 66 QWs, a redshift of the absorption peak at 70° can be observed. At grazing angle $\varphi=80°$ the redshift is substantial for thick MQW structures (10 meV with 100 wells), whereas this shift is barely noticeable in thin structures (with 33 QWs). A look at the maximum absorption value $A_{\max}$ of these spectra indicates that the traveling-wave approximation $A_{\max}\approx1-\exp(2N_{\mathrm{QW}}A_{\mathrm{QW}})$, where N_{QW} is the number of wells and A_{QW} is the absorption of one QW, does not apply when $\varphi\geqslant60°$. For example, at 60° and 70° incidence, the maximum absorption strength remains approximately unchanged between 66 and 100 wells.

The results for wafer *B* are displayed on Fig. 4. These spectra take into account the different Fresnel reflection losses between the perpendicular and in-plane polarizations. The values of φ are estimated within $\pm1.5°$ accuracy. Two main peaks are observed: a structure between 90 and 140 meV and a smooth absorption line centered at 210 meV. The latter comes from the intersubband transition $E1\rightarrow E3$. The reduced sensitivity of the $E1\rightarrow E3$ absorption line shape with respect to the incident angle φ is attributed to the small oscillator strength between these two states. The $E1\rightarrow E2$ absorption line centered at 100–110 meV evolves very quickly from 66° to 69°: the center of mass of the peak is redshifted and additional structures appear at low (~90 meV) and high frequencies (130–150 meV), i.e., in a spectral range where the absorption at the Brewster angle was negligible.[9] When adjusting the incident angle the position of the high-frequency peak can be tuned continuously from 117 to 150 meV. As illustrated on Fig. 1, the $\varphi=66°-69°$ range corresponds to the situation where the spectral width of evanescent modes is very sensitive to the angle. At grazing angle (71.2°) a clear 10 meV redshift of the absorption peak is observed.

Simulations of these experimental results were performed by a multilayer calculation based on the transfer-matrix method in uniaxial materials. For the simulations these double (sample *A*) or step (sample *B*) quantum wells have been simplified to square quantum wells with a width L_{QW} compatible with the extent of the ground wave function. These square QWs have unity oscillator strength between the first two subbands and the energy separation E_{21} is 124 and 103 meV for samples *A* and *B*, respectively. The carrier concentration in the well is adjusted to fit the magnitude of the Brewster absorption, i.e., 4.2×10^{17} and $5\times10^{17}\,\mathrm{cm}^{-3}$ for samples *A* and *B*, respectively. The results are not very much influenced by the poorly defined QW effective thickness, since a larger L_{QW} would be compensated by a smaller average carrier concentration in the well. We note that the nonlocal effective-medium approach developed in Ref. 3 resolves this difficulty. The chosen Q factor of the intersubband oscillators corresponds to the measured FWHM of the Brewster absorption profiles ($Q=9$ and 10 for wafers *A* and *B*, respectively). The simulations are averaged over $\pm1°$ around the central angle φ to take into account the focusing of the IR beam. Even though the experimental angles φ are known within $\pm1.5°$ accuracy, we did not try to adjust the angle for better fits. The dielectric constants of the well and barrier are calculated using the classical models. We did not adjust any numerical values to fit the experimental results.

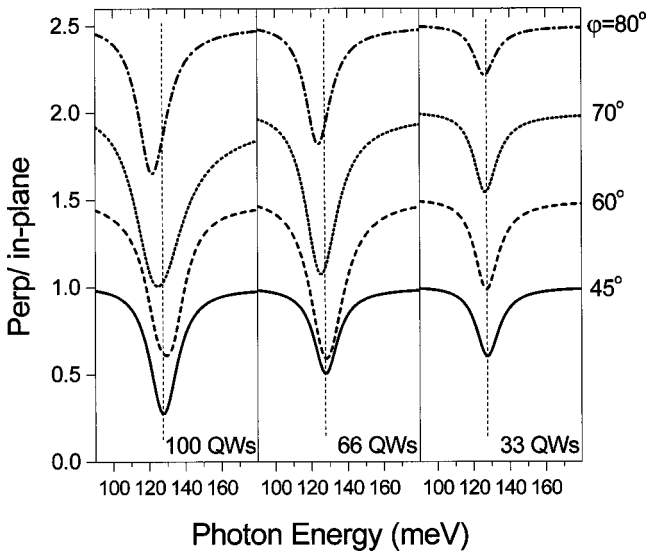

FIG. 5. Simulated transmittance spectra for wafer *A*. For clarity the spectra are vertically shifted by 0.5. The vertical dashed lines are drawn to guide the eye.

The results of these simulations are shown on Fig. 5 (sample *A*) and Fig. 6 (sample *B*). For sample *A*, the simulation fits the experimental spectra of Fig. 3 very well. The amount of redshift is exactly predicted for grazing angles and the magnitude of the calculated absorption agrees very well with the experimental data. Fitting the experimental results of wafer *B* with simulations was thought to be more challenging because of the numerous structures in the absorption spectra. Actually, the calculated absorption spectra as displayed on Fig. 6 from $\varphi=56°$ to 73° show a good agreement between experiments and theory. For instance, at $\varphi=70°-71°$ the predicted features at low (90 meV) and high (130–140 meV) frequency were observed experimentally at $\varphi=68.7°\pm1.5°$. We notice that the model suggests sharper structures than have been observed experimentally. One possible reason may come from the geometry of the 60° zigzag waveguide. Its length and thickness are not optimized for maximum throughput, which might result in a significant reflection of the IR beam at the output polished facet. Eventually, these reflected beams travel back to the MQWs, change the field profile inside the MQW, and, finally, randomize the absorption of the wells. Considering that no fitting parameter has been used, the simulations give a good prediction of the complex intersubband absorption in thick MQW structures.

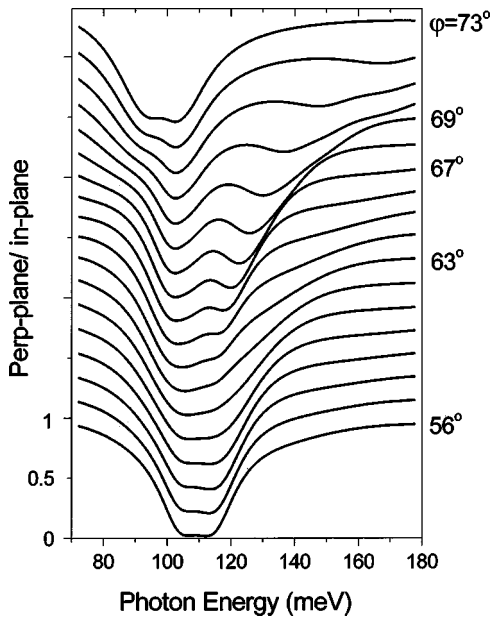

FIG. 6. Simulated transmittance spectra for wafer *B*. For clarity the spectra are vertically shifted by 0.2.

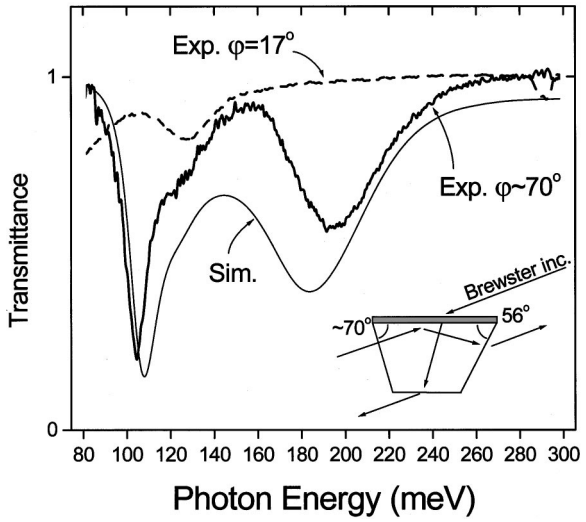

FIG. 7. Room-temperature transmittance spectra of wafer *C* at Brewster incidence ($\varphi=17°$, dashed line) and for $\varphi=70°$ (solid line). The thin-line curve is a simulation of the $\varphi=70°$ transmittance spectrum.

Finally, a QWIP structure was tested. Sample *C* is a 100-repeat square quantum-well structure. The well width is 66 Å, doped to an equivalent 2D density of $N_s=1.5\times10^{12}\,\mathrm{cm}^{-1}$, and the $Al_{0.192}Ga_{0.808}As$ barrier is 250 Å wide. The top and bottom n^+ GaAs contacting layers are 4000 and 8000 Å thick, respectively, and Si doped to 2×10^{18} cm^{-3}. The sample was polished into a prism: the entrance facet was polished for an internal incidence angle $\varphi=70°$ and the exit facet was polished at 56° to allow maximum throughput of *p*-polarized light (approximately the Brewster angle at the semiconductor/air interface). The experimental and theoretical spectra of the 70° waveguide are displayed on Fig. 7 as well as the transmittance for Brewster incidence ($\varphi=17°$). In accordance with absorption measurements at the Brewster angle, we used the following parameters for the simulation: $E_{21}=115.5\,\mathrm{meV}$, $Q=5.5$, and a 3D density $N_{3D}=1.4\times10^{18}\,\mathrm{cm}^{-3}$. Because our Lorentzian model is applied now to a case with bound-to-extended transition, N_{3D} is smaller than $N_s/(66\,\text{Å})$. Two absorption peaks are observed experimentally: an intense and narrow line at 104 meV and a broad feature at 195 meV. At the Brewster angle the absorption was too weak to be measurable at these photon energies. The predicted positions of the resonances (110 and 185 meV) are in close agreement with the experiment but the strength of absorption is overestimated by our model. We attribute this discrepancy to the bound-to-extended nature of the transitions, while our model uses an intersubband susceptibility based on a Lorentzian resonance. As seen with wafers *A* and *B*, this problem is less a concern with bound-to-bound transitions. We found that the 8000-Å-thick n^+ contact had to be

included in the model to simulate the peaks at 110 and 185 meV, indicating the influence of cavity effects above the substrate/n^+ GaAs critical angle. When tuning the incident angle we observed the position of the high-energy peak shifting very quickly, while the position of narrow peak stays almost unchanged. The simulations indicate that the high-energy peak (195 meV) corresponds to the situation where the radiation leaks into the MQW, i.e., φ is smaller than the substrate/n^+ GaAs critical angle when $\lambda < 6.4\,\mu$m. The low-energy peak (104 meV) corresponds to the coupling of the radiation into the waveguide formed by the MQW for the core and by the n^+ contact layers for the cladding.

To conclude, we have performed intersubband absorption measurements at grazing angles by using various multibounce waveguides. We have shown that above 45° incidence the traveling-wave approximation is invalid. The redshifts of the absorption peak observed at grazing angle and the surprising extra structures far detuned from the resonance can be explained by considering the well as a uniaxial absorbing material. We attribute these effects to the intersubband susceptibility, which induces evanescent waves inside the quantum wells and, consequently, significant multiple-reflection effects inside the MQW structure. We saw that the contacts in quantum-well infrared photodetector structures change the absorption significantly. This method of looking at the intersubband absorption might be important for optimization of grating-coupled quantum-well infrared photodetectors.

The authors thank Dr. Julien Nagle from the Laboratoire Central de Recherche, Thomson-CSF, for making the 200-repeat MQW sample available to this study. This work was supported in part by DND.

*Author to whom correspondence should be addressed. Electronic address: Duponte@ott.nrc.ca

[1] M. Helm, *Intersubband Transitions in Quantum Wells: Physics and Device Applications, Vol. 62 of Semiconductors and Semimetals*, edited by H. C. Liu and F. Capasso (Academic, San Diego, 2000).

[2] W. P. Chen, Y. J. Chen, and E. Burstein, Surf. Sci. **58**, 263 (1976).

[3] B. F. Levine, R. J. Malik, J. Walker, K. K. Choi, C. G. Bethea, D. A. Kleinman, and J. M. Vandenberg, Appl. Phys. Lett. **50**, 273 (1987).

[4] A. Seilmeier, H.-J. Hübner, G. Abstreiter, G. Welmann, and W. Schlapp, Phys. Rev. Lett. **59**, 1345 (1987).

[5] M. Załużny and C. Nalewajko, Phys. Rev. B **59**, 13 043 (1999).

[6] E. Dupont, D. Delacourt, and M. Papuchon, IEEE J. Quantum Electron. **29**, 2313 (1993).

[7] M. J. Kane, M. T. Emeny, N. Apsley, C. R. Whitehouse, and D. Lee, Semicond. Sci. Technol. **3**, 722 (1988).

[8] H. Schneider, C. Schönbein, M. Walther, P. Koidl, and G. Weimann, Appl. Phys. Lett. **74**, 16 (1999).

[9] H. C. Liu, E. Costard, E. Rosencher, and J. Nagle, IEEE J. Quantum Electron. **31**, 1659 (1995).

[10] K. L. Vodopyanov, K. O'Neill, G. B. Serapiglia, C. C. Phillips, M. Hopkinson, I. Vurgaftman, and J. R. Meyer, Appl. Phys. Lett. **72**, 2654 (1998).

[11] B. F. Levine, J. Appl. Phys. **74**, R1 (1993).

[12] S. Bandara, S. Gunapala, J. Liu, W. Hong, and J. Park, Proc. SPIE **2999**, 103 (1997).

[13] M. Załużny, Appl. Phys. Lett. **65**, 1817 (1994).